JCTC Journal of Chemical Theory and Computation

pubs.acs.org/JCTC Article

Understanding the Temperature Dependence and Finite Size Effects in Ab Initio MD Simulations of the Hydrated Electron

Sanghyun J. Park and Benjamin J. Schwartz*

Cite This: *J. Chem. Theory Comput.* 2022, 18, 4973−4982 Read Online

ACCESS | Metrics & More | Article Recommendations | Supporting Information

ABSTRACT: The hydrated electron is of interest to both theorists and experimentalists as a paradigm solution-phase quantum system. Although the bulk of the theoretical work studying the hydrated electron is based on mixed quantum/classical (MQC) methods, recent advances in computer power have allowed several attempts to study this object using *ab initio* methods. The difficulty with employing *ab initio* methods for this system is that even with relatively inexpensive quantum chemistry methods such as density functional theory (DFT), such calculations are still limited to at most a few tens of water molecules and only a few picoseconds duration, leaving open the question as to whether the calculations are converged with respect to either system size or dynamical fluctuations. Moreover, the *ab initio* simulations of the hydrated electron that have been published to date have provided only limited analysis. Most works calculate the electron's vertical detachment energy, which can be compared to experiment, and occasionally the electronic absorption spectrum is also computed. Structural features, such as pair distribution functions, are rare in the literature, with the majority of the structural analysis being simple statements that the electron resides in a cavity, which are often based only on a small number of simulation snapshots. Importantly, there has been no *ab initio* work examining the temperature-dependent behavior of the hydrated electron, which has not been satisfactorily explained by MQC simulations. In this work, we attempt to remedy this situation by running DFT-based *ab initio* simulations of the hydrated electron as a function of both box size and temperature. We show that the calculated properties of the hydrated electron are not converged even with simulation sizes up to 128 water molecules and durations of several tens of picoseconds. The simulations show significant changes in the water coordination and solvation structure with box size. Our temperature-dependent simulations predict a red-shift of the absorption spectrum (computed using TD-DFT with an optimally tuned range-separated hybrid functional) with increasing temperature, but the magnitude of the predicted red-shift is larger than that observed experimentally, and the absolute position of the calculated spectra are off by over half an eV. The spectral red-shift at high temperatures is accompanied by both a partial loss of structure of the electron's central cavity and an increased radius of gyration that pushes electron density onto and beyond the first solvation shell. Overall, although *ab initio* simulations can provide some insights into the temperature-dependent behavior of the hydrated electron, the simulation sizes and level of quantum chemistry theory that are currently accessible are inadequate for correctly describing the experimental properties of this fascinating object.

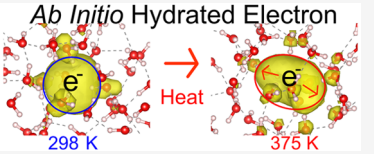

1. INTRODUCTION

The nature of the hydrated electron, an excess electron solvated by liquid water, is still the subject of debate despite its apparent simplicity. Until recently, much of the theoretical work studying the hydrated electron was based on mixed quantum/classical simulations, in which the electron is treated quantum mechanically but the water molecules are treated classically.[1−6] The structure and properties of the hydrated electron obtained in such simulations are highly sensitive to the pseudopotentials used to describe the electron−water interaction.[2,3,7] To date, most MQC simulations (but not all[3]) have concluded that the hydrated electron occupies a cavity in the water.[2,4,8] However, MQC simulations have been unable to explain all of the experimental properties of the hydrated electron, including the temperature dependence of the electron's absorption spectrum,[9−11] resonance Raman spectrum,[11,12] and molar solvation volume:[13,14] MQC models that predict some of these properties correctly usually fail dramatically in their predictions of the others.

Because of the failures of MQC models, recent efforts have focused on *ab initio* simulations of the hydrated electron. The first QM/MM treatment of the hydrated electron was described by Uhlig et al., who embedded 32 quantum mechanical water molecules and an excess electron in a box with 992 classical waters and ran dynamics using density functional theory (DFT) for the quantum subsystem.[15] The results yielded a hydrated electron with a somewhat fluxional structure[7,16] characterized by a central cavity that is smaller than those seen in traditional MQC simulations. The central cavity seen by Uhlig et al. contained only ∼40% of the excess electron's spin density.[15] A few years later, Ambrosio et al. ran

Received: April 7, 2022
Published: July 14, 2022

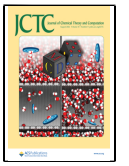

https://doi.org/10.1021/acs.jctc.2c00335
J. Chem. Theory Comput. 2022, 18, 4973−4982

ab initio dynamics using a hybrid DFT functional in a periodic system with 64 water molecules and an excess electron and also concluded that the electron occupies a cavity.[17] With certain approximations that will be discussed further below, these workers claimed that such simulations correctly predicted the experimental vertical detachment energy (VDE) and absorption spectrum of the hydrated electron.[17]

More recently, Wilhelm et al. performed *ab initio* simulations of the hydrated electron using the MP2 method.[18] Because MP2 is much more expensive than DFT, their calculations used DFT-based dynamics for five out of every six time steps, and were limited to a periodic box with only 47 water molecules and a total of ∼3 ps of dynamics.[18] Snapshots from this work show a cavity-like structure, but the computed bandgap was notably blue-shifted compared with the experimental absorption spectrum.[18] Using this MP2 model as a basis, the authors of ref 18 developed a neural network (NN)-based potential, enabling them to run longer trajectories.[19] The NN-based model also suggested that the structure of the hydrated electron is indeed cavity-like, but when nuclear quantum effects were added, the model generated configurations where the electron occasionally occupied a double cavity and also had an unusually wide range of VDEs that is not consistent with experiment.[19] Other *ab initio*[20,21] and QM/MM[22] simulations also have explored different aspects of the hydrated electron's behavior.

Although essentially every *ab initio* calculation has concluded that the hydrated electron is associated with a cavity in the water, no calculations presented to date have provided any detailed analysis or characterization of the electron's behavior. Occasionally, such work characterizes the electron's structure using pair distribution functions,[15,17] but there has been little discussion concerning the shape of the electron's wave function, its overlap with the surrounding water, or any fluctuations that may be crucial for understanding the temperature dependence.[16] Vertical detachment energies, which are perhaps the easiest value to extract from simulations that can be compared with experiment, are unfortunately not trivial to calculate in periodic systems that do not have a well-defined zero of energy. In addition, of computational necessity, *ab initio* simulations have been limited to very small system sizes, with little exploration of finite size effects.[17] Finite size effects have been shown to be important in MQC simulations of the hydrated electron with over 200 water molecules.[3] Thus, it is not clear whether *ab initio* simulations can truly capture the experimental properties of the hydrated electron, either due to inadequacies in the level of theory employed for the quantum mechanics (particularly DFT), the small system sizes that are computationally available, or both.

One of the most basic properties of the hydrated electron that has yet to be satisfactorily explained theoretically is its temperature dependence. Experiments have shown that the absorption spectrum of the hydrated electron red-shifts with increasing temperature by 2.2 meV/K, independent of the water density.[10] Moreover, spectral moment analysis indicates that the electron's radius of gyration increases at higher temperatures,[23] but the electron's molar solvation volume does not show any significant changes over the same temperature range.[14] This suggests that somehow the cavity structure associated with the hydrated electron is not strongly temperature dependent, but the diffuseness of its wave function and thus the overlap with the surrounding water increases as temperature is increased. MQC simulations in which the hydrated electron resides in a cavity do not show any temperature dependence (although a noncavity model does),[6,11] and to date, there has been no attempt to simulate the temperature dependence of the electron's properties using *ab initio* methods.

Thus, in this paper, we present a careful exploration of *ab initio* simulations of the hydrated electron to understand the roles of both finite size effects and temperature in the calculated structural and electronic properties. We perform DFT-based periodic simulations with box sizes of 47, 64, and 128 waters, and find that although the calculated VDE extrapolated to infinite box size is in good agreement with experiment, the structural and energetic properties of the hydrated electron are not converged even with 128 waters. We also explore the *ab initio* behavior of the hydrated electron at temperatures ranging from 298 to 375 K and calculate the spectroscopy using time-dependent density functional theory (TD-DFT) with an optimally tuned range-separated hybrid functional.[24] We find that the calculated spectrum indeed red-shifts with increasing temperature accompanied by only a modest change in the cavity structure, but the magnitude of the temperature-dependent spectral shift is overstated, and the simulated spectral shapes and positions do not agree well with experiment. We also fully characterize the hydrated electron's electronic and structural properties, allowing for a detailed comparison between different *ab initio* and MQC methods. We conclude that to date, no *ab initio* simulation method has had a high enough level of theory on a system of sufficient size to truly capture the nature of the hydrated electron.

2. METHODS

To perform *ab initio* molecular dynamics of the hydrated electron, we ran trajectories using the CP2K program suite.[25] We explored a total of five different systems with varying box sizes and temperatures. For the box size variation, periodic boxes containing 47, 64, and 128 water molecules at 298 K were used, and for the temperature dependence, we used the 64-water simulation box and explored temperature points at 298 K, 350 K and 375 K. Much of our work follows methodology that is largely similar to that previously published by Ambrosio et al.,[17] but with important differences as noted below. For running dynamics, we used the PBE0 functional with Grimme's DFT-D3 correction.[26] We note that CP2K uses Goedecker-Teter-Hutter pseudopotentials to represent core electrons, so only the valence electrons were accounted for in the quantum chemistry.[27] A triple-ζ quality basis set that is optimized to be used with the GTH pseudopotential (TZVP-GTH) was employed with a grid cutoff of 500 Ry; we verified that energy convergence was reached with this cutoff. The Hartree−Fock (HF) exchange in the DFT functional was calculated with a truncated scheme in which the cutoff was half of the box length. To accelerate the HF exchange calculation, the auxiliary density matrix method was employed with an auxiliary cFIT3 basis set.[28] All trajectories were propagated for at least 20 ps with a 0.5 fs time step in the NVT ensemble with the Nose-Hoover chain thermostat used to maintain the desired temperature.[29]

We set the system volume to give the experimental water density at room temperature and pressure, and held the density constant as the temperature was changed to exclude density-based effects from our analysis of the temperature dependence.[10,11,30] We note that the hydrated electron's spectrum shifts due to changes in both temperature and water density,[9]

https://doi.org/10.1021/acs.jctc.2c00335
J. Chem. Theory Comput. 2022, 18, 4973−4982

Table 1. Radius of Gyration, Direct Overlap (Θ, eq 2), Radial Overlap (Φ, eq 3), VDE, and Range Separation Parameter (ω) for All *ab Initio* Simulations of the Hydrated Electron Explored in This Work, Including Varying the Box Size and Temperature[a]

	64−298K	64−350K	64−375K	47−298K	128−298K	TB (298 K 500)
Radius of gyration (Å)	2.35 ± 0.09	2.54 ± 0.19	2.62 ± 0.24	2.34 ± 0.12	2.31 ± 0.08	2.42
Direct Overlap (%)	21.84 ± 2.16	21.01 ± 2.27	20.80 ± 2.52	21.99 ± 2.19	21.67 ± 2.13	5.7
Radial Overlap (%)	52.95 ± 3.31	55.95 ± 4.04	57.86 ± 4.92	53.14 ± 4.05	52.34 ± 3.60	31.1
VDE (eV)	2.14 ± 0.36	1.81 ± 0.37	1.95 ± 0.38	1.84 ± 0.35	2.35 ± 0.30	3.12
Optimal ω	0.175 a_0^{-1}	0.165 a_0^{-1}	0.160 a_0^{-1}	0.200 a_0^{-1}	0.185 a_0^{-1}	0.145 a_0^{-1}

[a]The quoted errors are ±1 standard deviation of the corresponding fluctuating quantity.

and at constant pressure, changing the temperature also simultaneously changes the density. Thus, to avoid confounding effects where multiple things that alter the spectrum change at the same time, we have chosen to compare to the experiments where the hydrated electron's spectrum was measured as a function of temperature at constant density, showing a redshift of 2.2 meV/K with increasing temperature.[10] Initial configurations were taken from an equilibrated MQC simulation using the cavity-forming Turi-Borgis pseudopotential,[2] and the first 5 ps of each ≥20 ps trajectory was not used for analysis to ensure equilibrium under *ab initio* propagation. Ensemble-averaged quantities were calculated using at least 100 uncorrelated configurations drawn every 100 fs for each system.

Surprisingly, there has been little work using *ab initio* simulations to calculate the absorption spectrum of the hydrated electron. The only such effort of which we are aware is that by Ambrosio et al.,[17] who simply binned the excited-state Kohn−Sham orbital energies from the periodic DFT calculation with respect to the ground-state energy to estimate the absorption spectrum; this procedure yielded what appears to be good agreement with experiment. We note, however, that if one calculates the absorption spectrum with excited states and transition dipole matrix elements from the TD-DFT calculations, the agreement with experiment becomes substantially worse because the spectrum becomes highly structured, as we document in the Supporting Information (SI). We also note that the application of standard hybrid functionals to the hydrated electron produces low-lying Kohn−Sham excited states with charge-transfer character, a general problem of charge delocalization that is well-known with DFT; these low-lying states were simply ignored in the work of Ambrosio et al., who used a radius-of-gyration-based criteria to select only those states that were confined near the central cavity for their spectral analysis.[17]

It is worth noting that previous work has shown that the level of theory used by Ambrosio et al. is expected to be inadequate for calculating the observed spectroscopy of the hydrated electron. In particular, the CP2K program only supports periodic TD-DFT calculations using the Tamm-Dancoff approximation,[31] which yields calculated spectra that do not conform with quantum mechanical sum rules used for the spectral moment analysis;[23] see SI Figure S4. Uhlig et al. have argued that when analyzing hydrated electron configurations generated from periodic simulations, it is important to use TD-DFT to calculate the excited states needed to generate a simulated absorption spectrum.[24] Moreover, these workers also showed that the calculated spectroscopy was extraordinarily sensitive to the choice of functional used in the calculation, and that the most reliable way to calculate the spectrum was to use TD-DFT with a range-separated hybrid functional, the range separation parameter of which was optimally tuned to satisfy Janak's theorem.[24,32]

Thus, for our calculations of the hydrated electron's absorption spectrum, we extracted uncorrelated configurations from our *ab initio* trajectories with the hydrated electron's center of mass set at the origin and performed nonperiodic TD-DFT calculations on these configurations using the QChem program suite.[33] To prevent the excess electron from spilling into the vacuum at the edges of the nonperiodically treated configurations, we surrounded the quantum mechanical waters with 26 replicated simulation boxes containing simple point charge (SPC) waters to represent the periodically treated water molecules. We chose the LRC-ωPBE functional, a range-separated version of the PBE functional used for the dynamics, for our spectral and other analyses; we found that this choice removed low-lying spurious charge-transfer excited states that are commonly observed with standard hybrid functionals such as PBE0, including those that had to be removed by Ambrosio et al.,[17] as discussed in the SI.

As suggested by Uhlig et al.,[24] we optimized the range separation parameter ω in the LRC-ωPBE functional to satisfy Janak's theorem[32] by taking uncorrelated configurations and determining the value of ω that led to the best average match of the ionization and SOMO energies for each of the five different simulation conditions. The optimized ω values that we employed are shown in the last row of Table 1, and details are given in the SI. It is worth noting that the optimized ω values are different for trajectories with different box sizes and temperatures, which shows that caution should be used if attempting to use the default ω value or when assuming that ω is roughly constant across different simulation conditions. For the TD-DFT calculations, we tested the convergence of the basis set (see the SI for details) and chose 6-31++G* as the best compromise between computational efficiency and accuracy.

Once the TD-DFT calculations for uncorrelated configurations from each condition were complete, we calculated the hydrated electron's absorption spectrum by taking the 10 lowest-lying TD-DFT excited states and binning them weighted by their oscillator strength, $|\mu_{0,i}|^2$, from the ground state. Each bin was then convoluted with the Gaussian kernel according to

$$I(E) = \left\langle \sum_{i=1}^{N} |\mu_{0,i}|^2 \Delta E_{0,i} \sqrt{\alpha/\pi} \exp(-\alpha(E - \Delta E_{0,i})^2) \right\rangle \quad (1)$$

where α was chosen to be 25 eV^{-2}, $\Delta E_{0,i}$ is the energy gap to the ith excited state, and the angled brackets represent an ensemble average. To verify this methodology, we also generated the absorption spectrum using configurations

https://doi.org/10.1021/acs.jctc.2c00335
J. Chem. Theory Comput. 2022, 18, 4973−4982

generated via MQC simulations using the cavity-forming TB potential,[2] which indeed do a reasonable job reproducing the experimental spectrum, as shown in the SI.[24] We used the SOMO generated from the TD-DFT calculations to best represent the hydrated electron's ground state in the various optical transitions, and we used the square of the TD-DFT SOMO to represent the ground-state charge density. We note that many other simulations have used the spin density for calculations and/or visualization,[15,18] but the spin density tends to have a larger radius of gyration than the square of the SOMO. This means that the radius of gyration of the electron based on the spin density will not be consistent with the sum rules used to determine the electron's size by spectral moment analysis,[23] as discussed in more detail in the SI.

3. RESULTS AND DISCUSSION

3.1. Finite Size Effects in *Ab Initio* Simulations of the Hydrated Electron. Although there has been a lot of *ab initio* work on water cluster anions,[34−37] which are precursors to the bulk hydrated electron, relatively little *ab initio* work to date aimed at simulating the bulk hydrated electron using periodic boundary conditions has been performed. The use of periodic boundary conditions, in turn, means that finite-size effects that alter the system properties could be important if the simulation box is too small.[3] However, the computational expense associated with *ab initio* dynamics severely limits the system size, with the largest equilibrium simulation to date by Ambrosio et al. having only 64 quantum mechanical water molecules.[17] In their work, Ambrosio et al. did perform limited calculations using a 128-water box, but they presented no analysis using the larger simulation size other than extracting a VDE to use in a two-point extrapolation to infinite box size.[17] We also note that Pizzochero et al. used DFT-based simulations to explore hydrated electron formation dynamics with a 128-water box,[20] but as far as we are aware, no *ab initio* simulations to date have examined the hydrated electron's equilibrium dynamics with a box containing more than 100 waters. As mentioned in the introduction, even MQC simulations of the hydrated electron show finite-size effects at box sizes greater than 200 waters,[3] much larger than what was used by Ambrosio et al. or the 47-water MP2-based simulations of Wilhelm et al.[17,18] Thus, in this section, we present a detailed exploration of how the simulation box size affects the calculated properties of periodic *ab initio* simulations of the hydrated electron.

To examine the effects of finite size, we used three different box sizes to simulate the hydrated electron containing 47, 64, and 128 water molecules. We begin our exploration of box size effects by examining the vertical detachment energy (VDE), which is perhaps the most easily computed quantity that can be directly compared to the ∼3.5 eV value measured experimentally.[38−40] We note, however, that calculating VDEs is not trivial when periodic boundary conditions are employed because there is no well-defined zero of energy; thus, the VDE cannot be simply computed as the difference in energy between neutral and anionic configurations. Because of this issue, Ambrosio et al. estimated the VDE from their simulations by integrating the SOMO energy by occupation and assuming that Janak's theorem holds for the hybrid functional employed in their simulations.[17] Since we used a similar hybrid functional as that employed by Ambrosio et al., we tested the accuracy of Janak's theorem but found that it does not hold. We also note that Ambrosio et al. shifted their calculated SOMO value by an an amount that was supposed to represent the energetic offset set from the water valence band edge;[17,41] however, these workers did not detail how they calculated this offset, and they did not report the value they used. Thus, without more information concerning precisely how the SOMO values were shifted, we believe that the excellent agreement reported between the simulated and experimental VDEs in their work is largely a coincidence.

To avoid the complexities of computing VDEs from periodic calculations, we computed the VDE using nonperiodic TD-DFT calculations on configurations extracted and extended from the periodic trajectories, as described above. Since we use a range-separated hybrid functional for these calculations that is optimally tuned to satisfy Janak's theorem, we can easily extract VDEs by taking the calculated SOMO energies, as shown in Table 1. We checked the validity of using the optimized long-range-corrected SOMO value by also computing the VDE by subtracting the energy of identical anionic and neutral configurations, and we obtained similar results, as shown in the SI. Table 1 shows that for all the system sizes we studied, including the 128-water box, the calculated VDEs are strikingly smaller than the experimental value. However, if we use the information from the three box sizes to extrapolate to infinite box size by plotting the calculated VDEs as a function of the inverse box length, we find better agreement with experiment, as shown in Figure 1. The fact that the calculated

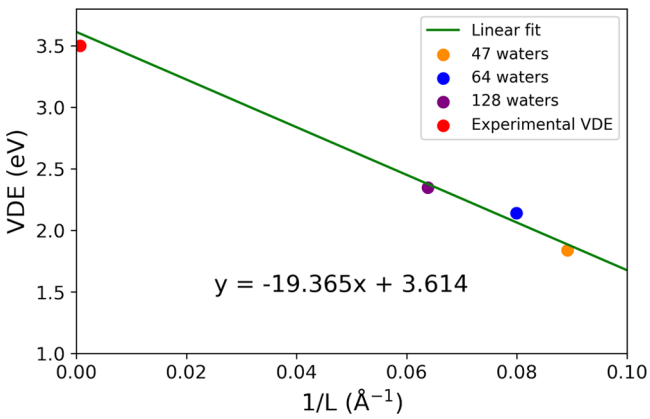

Figure 1. Vertical detachment energy of the hydrated electron calculated with nonperiodic TD-DFT using an optimally tuned range-separated hybrid functional on configurations extracted and extended from periodic *ab initio* simulations at three different box sizes, plotted against the inverse of the simulation box size. The ∼3.6 eV intercept of the best-fit line, which extrapolates the calculated VDEs to infinite box size, is in good agreement with experiment. However, the calculated VDE is more than an eV different from experiment even at the largest box size (Table 1), showing that 128 water molecules are not sufficient to converge the simulated properties of the hydrated electron.

VDE at the largest box size differs from experiment by well over an eV suggests that even with 128 waters, the simulations are not close to converged with respect to box size.

After the VDE, the next-easiest hydrated electron quantity that can be compared between simulation and experiment is the absorption spectrum. The absorption spectrum, however, is not terribly sensitive to the details of the hydrated electron's structure, as both cavity and noncavity MQC models with similar radii of gyration predict absorption spectra that are in good agreement with experiment.[2,3] The only *ab initio*

https://doi.org/10.1021/acs.jctc.2c00335
J. Chem. Theory Comput. 2022, 18, 4973−4982

simulation we are aware of that works to compute the hydrated electron's absorption spectrum is that by Ambosio et al.[17] As mentioned above, these workers calculated the spectrum by simply binning the energy differences between SOMO and unoccupied Kohn−Sham orbitals obtained directly from their periodic 64-water DFT-based simulation. They also manually removed the contributions of low-lying states by arguing that such states are likely an artifact from using DFT hybrid functionals.[17] When we perform similar periodic calculations using the PBE0 functional but using TD-DFT and computing transition dipoles between the states, the resulting absorption spectrum is strongly red-shifted, broadened, and more structured compared to experiment, as shown in the SI.

Due to these issues with using Kohn−Sham orbitals without transition dipoles to estimate the spectroscopy of the hydrated electron,[17] we elected to use TD-DFT calculations based on an optimally tuned range-separated hybrid functional, as outlined by Uhlig et al.,[24] and described above. The results for the three different box sizes we used at room temperature are shown as the yellow, blue, and purple curves in Figure 2a. We see that the spectral peak location does not appear to be terribly sensitive to the simulation box size, but the spectral shape and particularly width are box-size dependent. Moreover, the calculated absorption spectra are substantially blue-shifted and broadened compared both to experiment (thin black curve) and a standard cavity-model MQC simulation (thin pink curve).[2] Indeed, when we calculate the radius of gyration of the simulated hydrated electron (using the square of the TD-DFT SOMO), as shown in Table 1, we obtain an average value of ∼2.3 Å, which is substantially smaller than the 2.45 Å obtained experimentally through spectral moment analysis.[23] Since neither the radius or gyration nor the spectrum appear to be converging toward experiment with increasing box size, the representation of the hydrated electron with this level of theory is inadequate.

We analyze the structure associated with the hydrated electron via electron center-of-mass to water oxgyen pair distribution functions in Figure 2b. These are generated by using 150 independent, uncorrelated configurations for 47- and 64-water systems and 100 configurations for the 128-water system without any smoothing. We see that the *ab initio* hydrated electron (yellow, blue, and purple curves) is associated with a central cavity, but one in which the size is smaller and for which the solvation structure is more pronounced than that obtained from the standard cavity-forming Turi-Borgis MQC model (thin pink curve).[2] The height of the first-shell peak near 2.5 Å is also notably larger than that observed in the DFT-based QM/MM calculations of Uhlig et al. but the computed cavity size is similar.[15] Comparison with the 47-water MP2-based model by Wilhelm et al.[18] reveals that the MP2-based hydrated electron shows a somewhat more structured first solvation peak than our DFT-based model, as discussed in more detail in SI Figure S9. Interestingly, the *ab initio*-computed pair distribution functions do not show any significant size dependence, other than perhaps a slight decrease in the height and area of the second solvation shell near 4.5 Å with increasing box size. Electron center-of-mass to water H atom pair distribution functions, as well as several other structural characterizations of the hydrated electron, are shown in the SI.

To better delve into the structural changes that are responsible for the hydrated electron's VDE and spectral behavior with box size, we further examine aspects of the

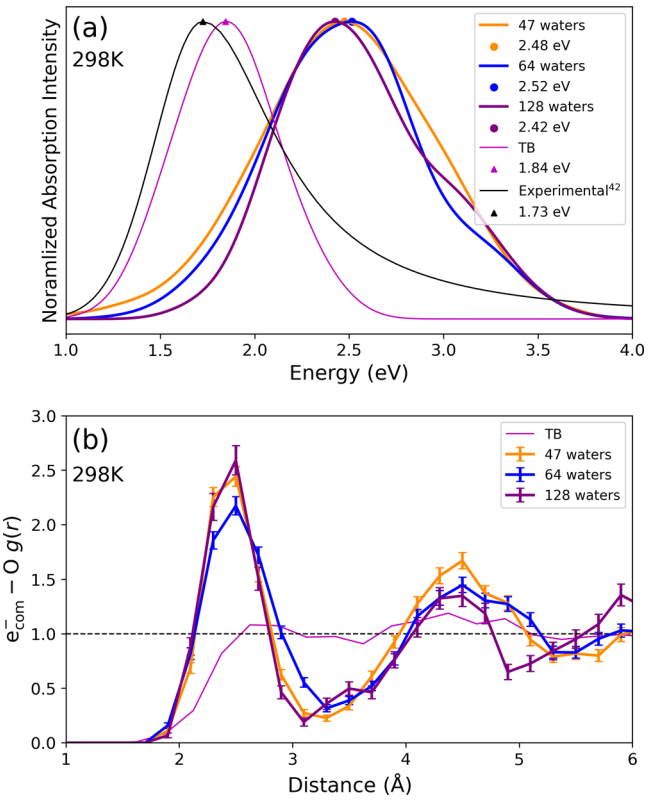

Figure 2. (a) Absorption spectrum of the hydrated electron calculated using configurations extracted and extended from periodic *ab initio* trajectories using TD-DFT with an optimally tuned range-separated hybrid functional using three different simulation sizes; the yellow, blue and brown curves represent simulation boxes with 47 (yellow curve), 64 (blue curve), and 128 (purple curve) H_2O molecules. The experimental absorption spectrum (taken from a Gauss-Lorentzian fit) at room temperature is shown as the thin black curve,[42,43] and the absorption spectrum calculated in the same manner using configurations taken from a MQC simulation run with the Turi-Borgis pseudopotential[2] is shown as the thin pink curve for reference. For the *ab initio* simulations, although the spectral position is not strongly size-dependent, the spectral width decreases with increasing box size due to a decrease in first-shell solvent coordination fluctuations (see text). The general agreement between the experimental and *ab initio*-generated spectra is poor. (b) Hydrated electron center-of-mass to water oxygen pair distribution functions, $g(r)$, at different *ab initio* simulation box sizes. The error bars represent 2 standard error deviations for each bin. The simulated structure around the central cavity is much more pronounced than in previous MQC simulations (thin pink curve), and monotonic box size effects are most prominent in the second solvation shell.

hydrated electron's structure in Figure 3. Here, we show the average e^-−water coordination number, defined as the number of water molecules whose oxygen atoms are within 3.5 Å of the electron's center-of-mass that also have an H atom within 2.5 Å of the center-of-mass; that is, the number of first-shell water molecules that are solvating the electron via H-bonding (see the SI for the corresponding angular distributions of the first-shell waters). For the 64-H_2O box, the average coordination number turns out to be ∼5, in good agreement with the observations of Ambrosio et al.[17] However, we also see that the degree of water coordination is highly box-size dependent. Both the smaller and particularly the larger box size show a stronger preference for electron coordination by only four waters. The larger fluctuations in coordination number in the

https://doi.org/10.1021/acs.jctc.2c00335
J. Chem. Theory Comput. 2022, 18, 4973−4982

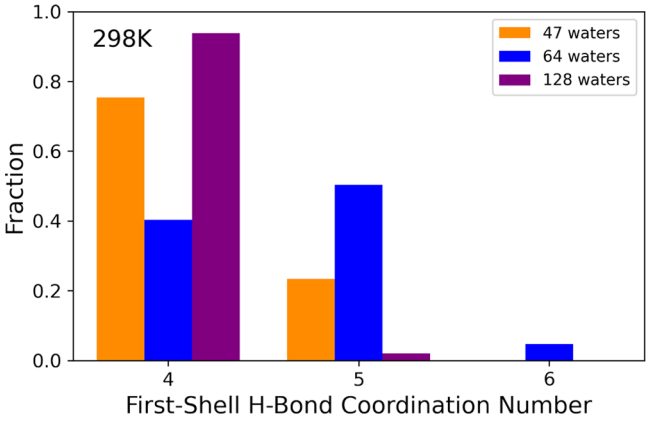

Figure 3. Fraction of *ab initio* hydrated electron configurations with different first-shell water coordination numbers (defined as those first-shell waters with H-bonds pointing at the electron's center-of-mass; see text) at different simulation box sizes. The coordination number does not show monotonic trends with system size. The average 5-coordination with 64 waters agrees with ref 17. For the largest 128-water box size, the coordination number is nearly precisely four with few fluctuations, possibly explaining the narrower absorption spectrum at this box size seen in Figure 2a.

smaller box sizes are likely the cause of the broader absorption spectra for these sizes seen in Figure 2a. The fact that we do not see a monotonic trend in coordination number with box size is another factor that suggests that structure of the electron is not converged even with the 128-water box.

To further characterize the behavior of the *ab initio* hydrated electron, we compute several quantities associated with its charge density. First, we examine the interactions between the electron and adjacent solvent molecules via the "direct overlap", Θ, given by[5,37,44]

$$\Theta = \left\langle \sum_{i=1}^{n_{\text{molcs}}} 4\pi \int_0^{r_c} r_i^2 |\Psi(r_i)|^2 \, \mathrm{d}r_i \right\rangle \tag{2}$$

where the angled brackets represent an ensemble average, Ψ is the normalized TD-DFT-calculated SOMO using the optimized range-separated hybrid functional, the sum runs over all of the water molecules, r_i is the distance between the electron and the ith water oxygen atom, and r_c is a constant that roughly represents the size of the water molecular core orbitals, here chosen to be 1.0 Å.[5] The direct overlap thus represents the fraction of the hydrated electron's charge density that lies directly on top of (as opposed to in between) the surrounding water molecules; the results for different simulation sizes are given in Table 1. Within error, there is no box size dependence to the direct overlap, but what is striking is that the *ab initio* value of Θ ∼ 21% is much larger than the ∼6% obtained from cavity-model MQC simulations, suggesting that the pseudopotentials used in such simulations are much too repulsive.[5,7,16,37]

Given that roughly 21% of the *ab initio* hydrated electron sits directly on top of the water, it is also interesting to determine what fraction of the electron sits out of the central cavity between the water molecules. To quantify this, we computed the "radial overlap", Φ, defined as[5]

$$\Phi = 4\pi \int r^2 g(r) |\Psi(r)|^2 \mathrm{d}r \tag{3}$$

where $g(r)$ is the electron center-of-mass to water oxygen pair distribution function (cf. Figure 2b). With this definition, Φ measures the fraction of the electron's charge density that resides at the same distance from the electron's center-of-mass as the surrounding water molecules; the difference between this value and 100% roughly gives the fraction of the electron that resides in the central cavity. Values of Φ for the different simulation box sizes are given in Table 1. For all box sizes, the radial overlap is roughly 53%, meaning that less than half of the electron resides in the central cavity, a result in decent agreement with previous QM/MM estimates based on the spin density.[15] The amount of radial overlap is much larger than the ∼30% seen in cavity-model MQC simulations, again consistent with the idea that the pseudopotentials used in such simulations overly confine the electron to the central cavity.[5,16,37] In the SI, we show several other measures of the cavity nature of the hydrated electron, along with measures of the shape of the electron's wave function.

Overall, the fact that few of the structural quantities we calculate are strongly dependent on box size makes it difficult to determine why the VDE appears to converge to the experimental value when extrapolated to infinite box size. Clearly, long-range electrostatic forces help to stabilize the hydrated electron, but given that the Onsager length in room-temperature water is only ∼7 Å, long-range electrostatics is not enough to fully explain the behavior of the VDE with box size. The change in water coordination number might be responsible, but the observation that the average coordination number decreases in the largest box size indicates that there must be subtleties in the number of coordinating water molecules and the strength with which they stabilize the hydrated electron. All of the results indicate that even 128 waters are not enough to converge the simulated properties of the hydrated electron. The simulated spectroscopy of the electron agrees poorly with experiment at all box sizes, suggesting that the level of theory chosen for the dynamics based on a hybrid DFT functional is likely inadequate. This is perhaps not surprising as it is hard to imagine a single hybrid functional correctly representing the valence electrons in the water molecular orbitals, the water−water H-bonds, water−water dispersion interactions, and the excess electron, of which ∼79% sits in the cavity and interstitial spaces between the water molecules. With MP2 and other wave function methods currently out of reach for the necessary simulation sizes and durations, there is clearly work to be done to describe the bulk hydrated electron using *ab initio* MD simulations.

3.2. Temperature Effects on the Hydrated Electron.

As discussed in the Introduction, the temperature dependence of the hydrated electron's absorption spectrum has never been satisfactorily explained by theory. Noncavity MQC simulations that do show a temperature-dependence reminiscent of experiment predict the wrong sign for the electron's molar solvation volume, while cavity MQC simulations that get the molar solvation volume about right do not show any temperature dependence whatsoever.[6,11] Although the analysis above suggests that *ab initio* simulations based on a hybrid DFT functional with a small number of waters are likely not up to the task, it is still instructive to see if this level of theory can explain why the radius of gyration of the electron increases with temperature[9] but the molar solvation volume, which is presumably closely connected to the cavity size, does not.[14] Thus, we ran simulations with 64 waters at fixed density at three different temperatures, 298, 350, and 375 K, to draw

https://doi.org/10.1021/acs.jctc.2c00335
J. Chem. Theory Comput. 2022, 18, 4973−4982

insights into what features of *ab initio*-simulated hydrated electrons change with temperature.

Figure 4a shows the calculated absorption spectrum of the *ab initio* hydrated electron, using the same optimized range-separated hybrid functional TD-DFT methodology described above, at the three different temperatures. The most striking feature of this data is that there is indeed a nearly 200 meV red-shift of the calculated absorption spectrum as the temperature is increased from 298 to 375 K. Although the absolute positions of the calculated spectra do not match experiment, the magnitude of the *T*-dependent shift of the absorption maximum is comparable to (but larger) than that observed experimentally.[10] The data also show, however, that the width of the calculated spectrum, which is already too broad at room temperature, increases even further at higher temperatures, a feature that is not observed in experiment.[9] There are also significant *T*-dependent changes in the calculated spectral shape, with the shoulder on the blue side at room temperature becoming a shoulder on the red side as *T* is increased (and of course, there are no shoulders present in the experimental spectrum of the hydrated electron). Thus, even though the basic temperature-dependent red-shift is in rough agreement with experiment, the spectral details are in rather poor agreement.

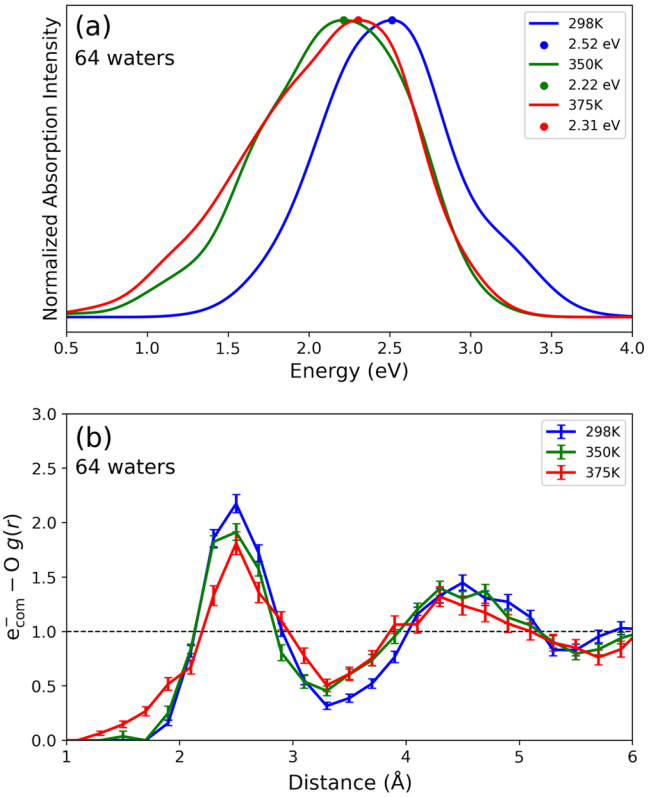

Figure 4. (a) Optimally tuned range-separated hybrid functional TD-DFT-calculated *ab initio* absorption spectrum of the hydrated electron at three different temperatures: 298 K (blue curve), 350 K (green curve), and 375 K (red curve). Although the spectra are in the wrong position and are broader than experiment, the magnitude of the observed red-shift with temperature is comparable to (but about twice as large as) that seen experimentally. (b) Electron center-of-mass to water oxygen pair distribution functions at different temperatures. The error bars represent 2 standard error deviations for each bin. Increasing temperature moves waters from the well-defined first solvation shell both into the central cavity and into the interstitial space between the first and second solvation shells.

To understand how the observed red-shift of the *ab initio* hydrated electron's spectrum is connected to its underlying structure, in Figure 4b we show electron center-of-mass to water oxygen pair distribution functions at the three different simulation temperatures. As the temperature is increased, we see that the first-shell solvation peak decreases in amplitude and increases in width, while the interstitial space between the first and second shells slightly fills in. This suggests that at higher temperatures, the first-shell waters are much more fluxional and thus more likely to reside either slightly closer to or farther from the electron's center-of-mass. Perhaps most importantly, there is significant penetration of waters into the central cavity at the highest temperature, suggesting that the spectral properties indeed reflect the nature of a *T*-dependent central cavity structure.[6,16]

Additional detail about how the solvent coordination changes with temperature is given in Figure 5. Panel a shows that as the temperature is increased, the most prominent coordination number shifts from 5 to 4. This results from the facts that there are both fewer first-shell waters and that fewer of the first-shell waters maintain a favorable H-bonding geometry with the hydrated electron at higher temperatures. The change in the prevalence of favorable H-bonds with temperature is shown in Figure 5b, which tabulates the number of first-shell coordinating waters that make either 1 or 2 H-bonds to the hydrated electron. The data clearly show an increase in the number of doubly coordinating waters with increasing temperature, indicating that the structure of the cavity and the local water H-bond network are becoming less well-defined. This idea is extended in Figure 5c, which shows the angular distribution of the first-shell water O−H bonds relative to the electron's center of mass for 4-coordinate configurations. As temperature increases, the distribution not only broadens, but shifts to lower angles, indicating that there is less preference for a tetrahedral H-bond geometry[37,45] and thus a higher likelihood to find dipole solvation or other motifs. It is the combination of the change in number of first-shell molecules and their angular distribution that results in the broadening and shape change of the simulated spectrum with temperature.

To understand how the temperature-dependent changes in the local water structure affect the electronic properties of the hydrated electron, we also analyzed the radius of gyration and the direct (Θ, eq 2) and radial (Φ, eq 3) water overlaps,[5] all of which are summarized in Table 1. As expected, the electron's radius of gyration is roughly inversely correlated with the position of the absorption spectrum and monotonically increases with temperature. More surprisingly, the direct overlap slightly decreases with increasing temperature; apparently, the greater conformational space available to the nearby waters at higher temperatures allows them to avoid enthalpically unfavorable overlap interactions with the electron. The radial overlap, in contrast, increases with increasing temperature for two reasons. First, the increased radius of gyration puts more of the solvated electron outside the central cavity and into the region between the first and second solvation shells. Second, the radial overlap also increases because the water penetrates into the central cavity region at high temperatures. Taken together, the results all suggest that the structure that defines the cavity containing the hydrated electron weakens with increasing temperature. The

https://doi.org/10.1021/acs.jctc.2c00335
J. Chem. Theory Comput. 2022, 18, 4973−4982

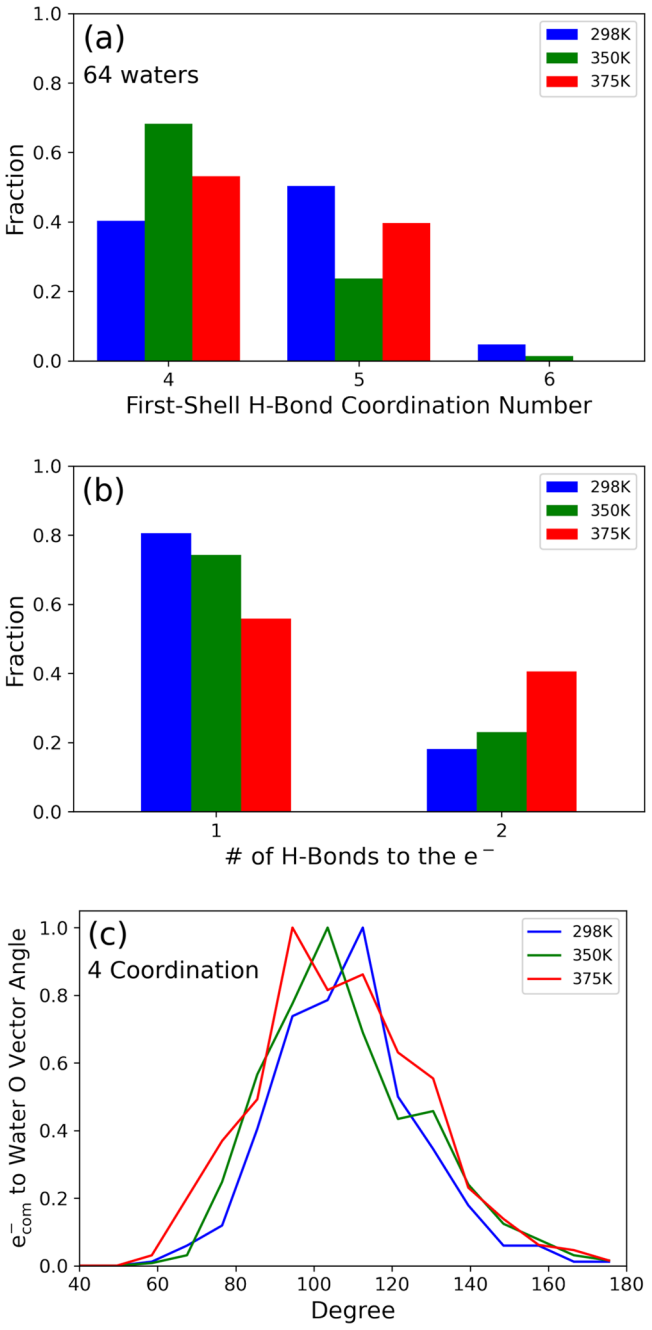

Figure 5. (a) Fraction of *ab initio* hydrated electron configurations with different first-shell water coordination numbers (defined as those first-shell waters with H-bonds pointing at the electron's center-of-mass; see text) at different simulation temperatures. As the temperature increases, the average coordination number at first decreases due to increased entropy, and then increases because the number of waters close to the electron's center-of-mass increases (cf. Figure 4b). (b) Fraction of first-shell waters making either 1 or 2 H-bonds to the hydrated electron at different temperatures. The number of waters making 2 H-bonds (dipole solvation rather than H-bond solvation) increases with increasing temperature, again the result of increased entropy. This effect also contributes to the increase in 5-coordination observed at the highest temperature. (c) Angle distribution between vectors connecting electron's center-of-mass (ecom) and the water oxygen atoms of the first-shell waters for 4-coordinate configurations at 3 different temperatures. The angular distribution, which is largely tetrahedral at room temperature, becomes both broader and less tetrahedral as the temperature increases.

central cavity remains roughly the same size, however, so that the simulations are roughly consistent with the experimental observations that the radius of gyration increases with temperature,[9] but the molar solvation volume is roughly temperature independent.[14]

Finally, Table 1 also shows that the calculated VDE decreases with increasing temperature. This prediction is in sharp contrast to traditional MQC cavity models of the hydrated electron, which show no change in VDE or absorption spectrum with temperature.[2,11] The decreased VDE of the *ab initio* hydrated electron reflects the lower coordination number and loss of the well-defined stabilizing H-bonded solvation structure, as well as the increased radius of gyration, as the temperature increases. Although the computed temperature-dependent VDE decrease is only ∼200 meV between 298 and 375 K, the fact that our 64-water simulations are not converged with respect to box size means that the VDE change with temperature extrapolated to infinite box size would likely be larger, and thus measurable by experiment. As far as we are aware, the hydrated electron's VDE has only been measured at room temperature,[40] so the roughly few-hundred meV decrease in VDE with increasing temperature over water's stability range at 1 atm is a prediction of this work.

4. CONCLUSIONS

In summary, we have shown that periodic *ab initio* simulations of the hydrated electron are not converged, even for our largest box containing 128 H_2O DFT-treated water molecules. The calculated VDE is still over an eV lower than experiment at this box size, although the agreement with experiment improves when the calculated value is extrapolated to infinite box size. When we use established methodology to calculate the hydrated electron's absorption spectrum using TD-DFT with an optimally tuned range-separated hybrid functional that suppresses spurious low-lying excited states and accounts for the transition dipoles between the ground and different excited states, the agreement with experiment is poor. The calculated absorption maximum is off by more than 0.5 eV, the calculated spectral width is too large, and the calculated spectrum shows structure that is not seen experimentally. This suggests that the configurations generated by this level of theory are likely not correctly representative of those of the experimental object.

One reason for the failure of this level of theory to correctly capture the behavior of the hydrated electron are excessive fluctuations that occur with small system sizes. Both $g(r)$ and the H-bond coordination of the hydrated electron change nonmonotonically with system size, at least up to 128 waters, indicating that simulations at this size are likely not converged. The magnitude of the fluctuations observed in the first-shell solvation structure is large at small system sizes, but these fluctuations appear to decrease in simulations with 128 waters, so it is possible that the size needed to accurately capture the properties of the hydrated electron may only be a few hundred waters, provided that the level of electronic structure theory used is up to the task.

One interesting feature is that our *ab initio* model is qualitatively able to reproduce the red-shift of the hydrated electron's absorption spectrum with increasing temperature. Although many spectral details, such as the spectral position, broadness, and spectral structure do not match experiment, the simulations do predict a net spectral red-shift as the temperature increases from 298 to 375 K at constant density. The magnitude of the predicted redshift is roughly double that

https://doi.org/10.1021/acs.jctc.2c00335
J. Chem. Theory Comput. 2022, 18, 4973−4982

seen experimentally, consistent with the idea that the small simulation box size produces configurations that are too fluxional. The simulated red-shift results from an increase in the electron's radius of gyration at higher temperatures, which occurs because some of the ∼47% of the electron density in the central cavity at room temperature moves out into the region occupied by the first shell waters and beyond. The water structure around the central cavity becomes less well-defined, but the cavity size is mostly maintained at higher temperatures, which is consistent with the observation that the molar solvation volume of the electron is roughly temperature independent over this range.[14] Thus, to the extent that these simulations do reflect experiment, the temperature dependence of the hydrated electron's properties results primarily from changes in the water structure around the central cavity: in other words, fluctuations are important.[6,16,37]

Overall, despite this qualitative agreement with experiment, all of the results indicate that *ab inito* simulations still have a ways to go to properly explain the properties of the hydrated electron. DFT-based simulations have a tough time getting the structure and dynamics of liquid water correct,[46,47] so the properties of water in the presence of an excess electron, where fine details of the structure, dynamics, and fluctuations are critical to understanding experiment, are still a challenge for this level of theory, particularly given that at least a few hundred waters and many tens of picoseconds are needed for convergence. Comparing the VDE obtained from periodic simulations that do not have a well-defined zero of energy to experiment requires approximations that have not been well tested, although our use of an optimally tuned range-separated hybrid functional at least seems to extrapolate well to the experimental value. Comparing the calculated absorption spectrum to experiment is also not straightforward, particularly given the difficulty of obtaining meaningful excited states even with TD-DFT. The way that transition dipoles and potentially spurious excited states result from the charge delocalization error inherent with DFT also presents challenges. We believe that better benchmarking for this class of simulations is needed to ensure that the results obtained are experimentally relevant and do not simply agree by coincidence.

■ ASSOCIATED CONTENT

Supporting Information

The Supporting Information is available free of charge at https://pubs.acs.org/doi/10.1021/acs.jctc.2c00335.

Parameters used in the simulation, additional details of the simulations methodology, and additional data analysis (PDF)

■ AUTHOR INFORMATION

Corresponding Author

Benjamin J. Schwartz − *Department of Chemistry and Biochemistry, University of California,Los Angeles, Los Angeles, California 90095-1569, United States;* orcid.org/0000-0003-3257-9152; Email: schwartz@chem.ucla.edu

Author

Sanghyun J. Park − *Department of Chemistry and Biochemistry, University of California,Los Angeles, Los Angeles, California 90095-1569, United States*

Complete contact information is available at: https://pubs.acs.org/10.1021/acs.jctc.2c00335

Notes

The authors declare no competing financial interest.

■ ACKNOWLEDGMENTS

This work was supported by the National Science Foundation under Grant Number CHE-1856050. Computational resources were provided by the UCLA Institute for Digital Research and Education and by XSEDE under computational project TG-CHE170065.

■ REFERENCES

(1) Turi, L.; Gaigeot, M.-P.; Levy, N.; Borgis, D. Analytical investigations of an electron-water molecule pseudopotential. I. Exact calculations on a model system. *J. Chem. Phys.* **2001**, *114*, 7805−7815.

(2) Turi, L.; Borgis, D. Analytical investigations of an electron-water molecule pseudopotential. II Development of a new pair potential and molecular dynamics simulations. *J. Chem. Phys.* **2002**, *117*, 6186−6195.

(3) Larsen, R. E.; Glover, W. J.; Schwartz, B. J. Does the hydrated electron occupy a cavity? *Science* **2010**, *329*, 65−69.

(4) Jacobson, L. D.; Herbert, J. M. A one-electron model for the aqueous electron that includes many-body electron-water polarization: Bulk equilibrium structure, vertical electron binding energy, and optical absorption spectrum. *J. Chem. Phys.* **2010**, *133*, 154506.

(5) Casey, J. R.; Kahros, A.; Schwartz, B. J. To be or not to be in a cavity: the hydrated electron dilemma. *J. Phys. Chem. B* **2013**, *117*, 14173−14182.

(6) Zho, C.-C.; Farr, E. P.; Glover, W. J.; Schwartz, B. J. Temperature dependence of the hydrated electron's excited-state relaxation. I. Simulation predictions of resonance Raman and pump-probe transient absorption spectra of cavity and non-cavity models. *J. Chem. Phys.* **2017**, *147*, 074503.

(7) Glover, W. J.; Schwartz, B. J. Short-range electron correlation stabilizes noncavity solvation of the hydrated electron. *J. Chem. Theory Comput.* **2016**, *12*, 5117−5131.

(8) Schnitker, J.; Rossky, P. J. Quantum simulation study of the hydrated electron. *J. Chem. Phys.* **1987**, *86*, 3471−3485.

(9) Bartels, D. M.; Takahashi, K.; Cline, J. A.; Marin, T. W.; Jonah, C. D. Pulse radiolysis of supercritical water. 3 Spectrum and thermodynamics of the hydrated electron. *J. Phys. Chem. A* **2005**, *109*, 1299−1307.

(10) Du, Y.; Price, E.; Bartels, D. M. Solvated electron spectrum in supercooled water and ice. *Chemical physics letters* **2007**, *438*, 234−237.

(11) Casey, J. R.; Larsen, R. E.; Schwartz, B. J. Resonance Raman and temperature-dependent electronic absorption spectra of cavity and noncavity models of the hydrated electron. *Proc. Natl. Acad. Sci. U. S. A.* **2013**, *110*, 2712−2717.

(12) Tauber, M. J.; Mathies, R. A. Resonance Raman spectra and vibronic analysis of the aqueous solvated electron. *Chemical physics letters* **2002**, *354*, 518−526.

(13) Borsarelli, C. D.; Bertolotti, S. G.; Previtali, C. M. Thermodynamic changes associated with the formation of the hydrated electron after photoionization of inorganic anions: a time-resolved photoacoustic study. *Photochemical & Photobiological Sciences* **2003**, *2*, 791−795.

(14) Janik, I.; Lisovskaya, A.; Bartels, D. M. Partial molar volume of the hydrated electron. *J. Phys. Chem. Lett.* **2019**, *10*, 2220−2226.

(15) Uhlig, F.; Marsalek, O.; Jungwirth, P. Unraveling the complex nature of the hydrated electron. *J. Phys. Chem. Lett.* **2012**, *3*, 3071−3075.

(16) Glover, W. J.; Schwartz, B. J. The fluxional nature of the hydrated electron: energy and entropy contributions to aqueous electron free energies. *J. Chem. Theory Comput.* **2020**, *16*, 1263−1270.

(17) Ambrosio, F.; Miceli, G.; Pasquarello, A. Electronic levels of excess electrons in liquid water. *journal of physical chemistry letters* **2017**, *8*, 2055−2059.

(18) Wilhelm, J.; VandeVondele, J.; Rybkin, V. V. Dynamics of the Bulk Hydrated Electron from Many-Body Wave-Function Theory. *Angew. Chem., Int. Ed.* **2019**, *58*, 3890−3893.
(19) Lan, J.; Kapil, V.; Gasparotto, P.; Ceriotti, M.; Iannuzzi, M.; Rybkin, V. V. Simulating the ghost: quantum dynamics of the solvated electron. *Nat. Commun.* **2021**, *12*, 1−6.
(20) Pizzochero, M.; Ambrosio, F.; Pasquarello, A. Picture of the wet electron: a localized transient state in liquid water. *Chemical science* **2019**, *10*, 7442−7448.
(21) Dasgupta, S.; Rana, B.; Herbert, J. M. Ab initio investigation of the resonance Raman spectrum of the hydrated electron. *J. Phys. Chem. B* **2019**, *123*, 8074−8085.
(22) Shen, Z.; Peng, S.; Glover, W. J. Flexible boundary layer using exchange for embedding theories. II. QM/MM dynamics of the hydrated electron. *J. Chem. Phys.* **2021**, *155*, 224113.
(23) Bartels, D. M. Moment analysis of hydrated electron cluster spectra: Surface or internal states? *J. Chem. Phys.* **2001**, *115*, 4404−4405.
(24) Uhlig, F.; Herbert, J. M.; Coons, M. P.; Jungwirth, P. Optical spectroscopy of the bulk and interfacial hydrated electron from ab initio calculations. *J. Phys. Chem. A* **2014**, *118*, 7507−7515.
(25) Hutter, J.; Iannuzzi, M.; Schiffmann, F.; VandeVondele, J. cp2k: atomistic simulations of condensed matter systems. *Wiley Interdisciplinary Reviews: Computational Molecular Science* **2014**, *4*, 15−25.
(26) Grimme, S.; Antony, J.; Ehrlich, S.; Krieg, H. A consistent and accurate ab initio parametrization of density functional dispersion correction (DFT-D) for the 94 elements H-Pu. *J. Chem. Phys.* **2010**, *132*, 154104.
(27) Goedecker, S.; Teter, M.; Hutter, J. Separable dual-space Gaussian pseudopotentials. *Phys. Rev. B* **1996**, *54*, 1703.
(28) Guidon, M.; Hutter, J.; VandeVondele, J. Auxiliary density matrix methods for Hartree- Fock exchange calculations. *J. Chem. Theory Comput.* **2010**, *6*, 2348−2364.
(29) Martyna, G. J.; Klein, M. L.; Tuckerman, M. Nosé-Hoover chains: The canonical ensemble via continuous dynamics. *J. Chem. Phys.* **1992**, *97*, 2635−2643.
(30) Nicolas, C.; Boutin, A.; Lévy, B.; Borgis, D. Molecular simulation of a hydrated electron at different thermodynamic state points. *J. Chem. Phys.* **2003**, *118*, 9689−9696.
(31) Janak, J. F. Proof that $\partial E/\partial n_i=\epsilon$ in density-functional theory. *Phys. Rev. B* **1978**, *18*, 7165.
(32) Hirata, S.; Head-Gordon, M. Time-dependent density functional theory within the Tamm-Dancoff approximation. *Chem. Phys. Lett.* **1999**, *314*, 291−299.
(33) Shao, Y.; Gan, Z.; Epifanovsky, E.; Gilbert, A. T.B.; Wormit, M.; Kussmann, J.; Lange, A. W.; Behn, A.; Deng, J.; Feng, X.; Ghosh, D.; Goldey, M.; Horn, P. R.; Jacobson, L. D.; Kaliman, I.; Khaliullin, R. Z.; Kus, T.; Landau, A.; Liu, J.; Proynov, E. I.; Rhee, Y. M.; Richard, R. M.; Rohrdanz, M. A.; Steele, R. P.; Sundstrom, E. J.; Woodcock, H. L.; Zimmerman, P. M.; Zuev, D.; Albrecht, B.; Alguire, E.; Austin, B.; Beran, G. J. O.; Bernard, Y. A.; Berquist, E.; Brandhorst, K.; Bravaya, K. B.; Brown, S. T.; Casanova, D.; Chang, C.-M.; Chen, Y.; Chien, S. H.; Closser, K. D.; Crittenden, D. L.; Diedenhofen, M.; DiStasio, R. A.; Do, H.; Dutoi, A. D.; Edgar, R. G.; Fatehi, S.; Fusti-Molnar, L.; Ghysels, A.; Golubeva-Zadorozhnaya, A.; Gomes, J.; Hanson-Heine, M. W.D.; Harbach, P. H.P.; Hauser, A. W.; Hohenstein, E. G.; Holden, Z. C.; Jagau, T.-C.; Ji, H.; Kaduk, B.; Khistyaev, K.; Kim, J.; Kim, J.; King, R. A.; Klunzinger, P.; Kosenkov, D.; Kowalczyk, T.; Krauter, C. M.; Lao, K. U.; Laurent, A. D.; Lawler, K. V.; Levchenko, S. V.; Lin, C. Y.; Liu, F.; Livshits, E.; Lochan, R. C.; Luenser, A.; Manohar, P.; Manzer, S. F.; Mao, S.-P.; Mardirossian, N.; Marenich, A. V.; Maurer, S. A.; Mayhall, N. J.; Neuscamman, E.; Oana, C. M.; Olivares-Amaya, R.; O'Neill, D. P.; Parkhill, J. A.; Perrine, T. M.; Peverati, R.; Prociuk, A.; Rehn, D. R.; Rosta, E.; Russ, N. J.; Sharada, S. M.; Sharma, S.; Small, D. W.; Sodt, A.; Stein, T.; Stuck, D.; Su, Y.-C.; Thom, A. J.W.; Tsuchimochi, T.; Vanovschi, V.; Vogt, L.; Vydrov, O.; Wang, T.; Watson, M. A.; Wenzel, J.; White, A.; Williams, C. F.; Yang, J.; Yeganeh, S.; Yost, S. R.; You, Z.-Q.; Zhang, I. Y.; Zhang, X.; Zhao, Y.; Brooks, B. R.; Chan, G. K.L.; Chipman, D. M.; Cramer, C. J.; Goddard, W. A.; Gordon, M. S.; Hehre, W. J.; Klamt, A.; Schaefer, H. F.; Schmidt, M. W.; Sherrill, C. D.; Truhlar, D. G.; Warshel, A.; Xu, X.; Aspuru-Guzik, A.; Baer, R.; Bell, A. T.; Besley, N. A.; Chai, J.-D.; Dreuw, A.; Dunietz, B. D.; Furlani, T. R.; Gwaltney, S. R.; Hsu, C.-P.; Jung, Y.; Kong, J.; Lambrecht, D. S.; Liang, W.; Ochsenfeld, C.; Rassolov, V. A.; Slipchenko, L. V.; Subotnik, J. E.; Van Voorhis, T.; Herbert, J. M.; Krylov, A. I.; Gill, P. M.W.; Head-Gordon, M. Advances in molecular quantum chemistry contained in the Q-Chem 4 program package. *Mol. Phys.* **2015**, *113*, 184−215.
(34) Marsalek, O.; Uhlig, F.; Frigato, T.; Schmidt, B.; Jungwirth, P. Dynamics of electron localization in warm versus cold water clusters. *Physical review letters* **2010**, *105*, 043002.
(35) Frigato, T.; VandeVondele, J.; Schmidt, B.; Schütte, C.; Jungwirth, P. Ab initio molecular dynamics simulation of a medium-sized water cluster anion: From an interior to a surface-located excess electron via a delocalized state. *J. Phys. Chem. A* **2008**, *112*, 6125−6133.
(36) Zho, C.-C.; Vlĉek, V.; Neuhauser, D.; Schwartz, B. J. Thermal equilibration controls H-bonding and the vertical detachment energy of water cluster anions. *J. Phys. Chem. Lett.* **2018**, *9*, 5173−5178.
(37) Park, S. J.; Schwartz, B. J. Evaluating Simple Ab Initio Models of the Hydrated Electron: The Role of Dynamical Fluctuations. *J. Phys. Chem. B* **2020**, *124*, 9592−9603.
(38) Siefermann, K. R.; Liu, Y.; Lugovoy, E.; Link, O.; Faubel, M.; Buck, U.; Winter, B.; Abel, B. Binding energies, lifetimes and implications of bulk and interface solvated electrons in water. *Nature Chem.* **2010**, *2*, 274−279.
(39) Horio, T.; Shen, H.; Adachi, S.; Suzuki, T. Photoelectron spectra of solvated electrons in bulk water, methanol, and ethanol. *Chem. Phys. Lett.* **2012**, *535*, 12−16.
(40) Luckhaus, D.; Yamamoto, Y.-i.; Suzuki, T.; Signorell, R. Genuine binding energy of the hydrated electron. *Science advances* **2017**, *3*, e1603224.
(41) Ambrosio, F.; Miceli, G.; Pasquarello, A. Redox levels in aqueous solution: Effect of van der Waals interactions and hybrid functionals. *J. Chem. Phys.* **2015**, *143*, 244508.
(42) Hart, E. J.; Boag, J. W. Absorption spectrum of the hydrated electron in water and in aqueous solutions. *J. Am. Chem. Soc.* **1962**, *84*, 4090−4095.
(43) Jou, F.-Y.; Freeman, G. R. Temperature and isotope effects on the shape of the optical absorption spectrum of solvated electrons in water. *J. Phys. Chem.* **1979**, *83*, 2383−2387.
(44) Park, S. J.; Narvaez, W. A.; Schwartz, B. J. How Water-Ion Interactions Control the Formation of Hydrated Electron: Sodium Cation Contact Pairs. *J. Phys. Chem. B* **2021**, *125*, 13027−13040.
(45) Kumar, A.; Walker, J. A.; Bartels, D. M.; Sevilla, M. D. A simple ab initio model for the hydrated electron that matches experiment. *J. Phys. Chem. A* **2015**, *119*, 9148−9159.
(46) Gillan, M. J.; Alfe, D.; Michaelides, A. Perspective: How good is DFT for water? *J. Chem. Phys.* **2016**, *144*, 130901.
(47) Willow, S. Y.; Zeng, X. C.; Xantheas, S. S.; Kim, K. S.; Hirata, S. Why is MP2-water "cooler" and "denser" than DFT-water? *journal of physical chemistry letters* **2016**, *7*, 680−684.

https://doi.org/10.1021/acs.jctc.2c00335
J. Chem. Theory Comput. 2022, 18, 4973−4982